Extracting Macroscopic Stochastic Dynamics: Model Problems

WILHELM HUISINGA
Free University
CHRISTOF SCHÜTTE
Free University
AND
ANDREW M. STUART
University of Warwick

Abstract

The purpose of this work is to shed light on an algorithm designed to extract effective macroscopic models from detailed microscopic simulations. The particular algorithm we study is a recently developed transfer operator approach due to Schütte et al. [20]. The investigations involve the formulation, and subsequent numerical study, of a class of model problems. The model problems are ordinary differential equations constructed to have the property that, when projected onto a low-dimensional subspace, the dynamics is approximately that of a stochastic differential equation exhibiting a finite-state-space Markov chain structure. The numerical studies show that the transfer operator approach can accurately extract finite-state Markov chain behavior embedded within high-dimensional ordinary differential equations. In so doing the studies lend considerable weight to existing applications of the algorithm to the complex systems arising in applications such as molecular dynamics. The algorithm is predicated on the assumption of Markovian input data; further numerical studies probe the role of memory effects. Although preliminary, these studies of memory indicate interesting avenues for further development of the transfer operator methodology.

1 Introduction

Recently there have been significant advances in algorithms designed to extract effective macroscopic dynamics from detailed microscopic simulations [4, 20, 22]. They are based on the exploitation of spectral information from transfer operators that describe the overall dynamics of the system under consideration. The purpose of this work is to develop our understanding of these transfer-operator-based algorithms through the study of carefully chosen model problems.

The algorithms we study are used in the following situation. We are given a sequence $\{x_n\}$, $x_n \in X$, which is derived either from a deterministic problem (possibly with random data) or a stochastic problem. Here and below, the index $n \in$

Communications on Pure and Applied Mathematics, Vol. LVI, 0234–0269 (2003)

$\mathbb{Z}^+$. We assume that the *effective dynamics* of this sequence is given by statistically rare flips between a small number of *metastable sets* in phase space, while between the flips the sequence remains inside one of these metastable sets. Hence it is natural to try to represent the effective dynamics by a *finite-state Markov chain* that describes the flipping behavior between the metastable sets. This Markov chain will be called the *flipping chain*.

The aim is to find a projection Π onto a *low-dimensional* subspace Ω of X such that the sequence $\{q_n\} := \{\Pi x_n\} \subset \Omega$ exhibits metastable sets and an associated finite-state flipping chain that approximates the macroscopic dynamics of $\{x_n\}$. If this is achieved, then Π is the projection onto a set of *essential degrees of freedom* of the system given by $\{x_n\}$. When the sequence $\{x_n\} = \{x_n^\tau\}$ comes from a time-τ sampling of some continuous-time process, it is desirable that the effective dynamics be captured in the low-dimensional subspace Ω for *all* time-τ samplings. By introducing a family of model problems whose noise has memory with inverse correlation time scaling like a parameter α, we study this issue: We show examples where the approximation is good for sampling rate τ long compared to α^{-1}, but deteriorates for τ small relative to α^{-1}. In such a situation the effective dynamics is not properly captured, and further development of the transfer operator approach is called for.

Key Questions

The transfer operator approach to metastability has recently been developed as a mechanism for extracting macroscopic conformational information about molecules, starting from microscopic molecular dynamics data [5, 20]. The methodology employed to do this builds on related ideas developed for understanding deterministic dynamical systems [4]. Because the real molecular systems for which this approach has been applied are so complicated, a thorough understanding of some of the algorithmic issues that arise is difficult to achieve in that context. The goal of this work is to develop simple model problems and use them to study such algorithmic issues, especially the following questions:

(Q1) How should the low-dimensional subspace Ω, or equivalently the projection Π, be identified?

(Q2) Do the metastable sets and finite-state-space flipping chain corresponding to $\{q_n\}$ accurately represent the macroscopic dynamics of the $\{x_n\}$?

(Q3) In general, $\{q_n\}$ is not a Markov chain. What effect does memory have on the ability of the algorithm to correctly summarize the effective dynamics of $\{x_n\}$?

(Q4) In situations where memory has a significant detrimental effect on the predictive capabilities of the algorithm, how can the algorithm be improved?

Our Approach

The algorithmic approach to the identification of metastability [20] shows that metastable sets can be characterized by the dominant spectra of an appropriately

defined transfer operator: The dominant eigenvectors exhibit significant jumps at the boundary of the metastable sets but vary slowly within metastable sets. Thus the principal algorithmic idea relating to question (Q1) is that the *essential* degrees of freedom (locally) are characterized by projections in directions in which the dominant eigenvectors exhibit significant jumps. Conversely, the *nonessential* degrees of freedom are characterized as directions in which the dominant eigenvectors are *almost constant*. This allows a construction of the projection Π after identifying such directions. We will demonstrate that the simple model problems to be designed herein justify this construction of Π. We emphasize, however, that the dimension of X may sometimes be so high as to make the transfer operator approach to the identification of Π computationally infeasible if naively applied directly in X; this issue can be ameliorated to some extent by the use of adaptive algorithms such as those in [4, 8], but for many problems in high dimensions, combining the transfer operator approach with simpler clustering approaches and/or mathematical modeling, such as the exploitation of fast/slow time-scale separation, may be needed to identify Π.

In order to study question (Q2) we will assume that Π is known and examine the algorithmic approach of [20] when applied in Ω. We consider problems where a low-dimensional embedded Markov chain is known to exist. Specifically, we will study problems where X is of high dimension and the dynamics in Ω is approximately that of an Itô stochastic differential equation (SDE) in $\mathbb{R}$. Furthermore, we will assume that this SDE is of the type studied in [10] so that its dynamics may be approximated by a finite-state Markov chain by using large-deviation theory. The behavior of this Markov chain can then be compared with the flipping chain constructed algorithmically by the transfer operator approach.

Although examples may be found where elimination of many variables leads to an SDE in the remaining variables [9, 25], it is often the case that in this so-called Mori-Zwanzig approach, memory terms remain after the elimination [3]. To study question (Q3), we introduce model problems where the dynamics in Ω have significant memory; specifically, we have in Ω approximately the dynamics of a single component of an SDE in $\mathbb{R}^2$. As we will see, there may be no Markov chain in Ω that mimics the dynamics in Ω, but nevertheless the metastable sets predicted from studying the data in Ω do contain accurate information about the effective dynamics. However, the predictive capability may be compromised when memory is significant, and our experiments suggest interesting avenues for further development of the transfer operator methodology.

Model Problems

The systems we study are constructed from the flow of a deterministic ordinary differential equation (ODE) $\Phi^\tau : X \to X$ on a state space X, which is assumed to be decomposed according to $X = \Omega \times Z$, for instance, $X = \mathbb{R}^{2N+1} = \mathbb{R} \times \mathbb{R}^{2N}$. In this paper we concentrate on situations where the dynamics in Z evolve independently of those in Ω; specifically, the dynamics in Z will be the solution

of linear autonomous ODEs, namely harmonic oscillators. These will feed in as forcing for the dynamics in Ω. In a subsequent paper we will study problems with full coupling between the Ω and Z dynamics; in particular, we will study problems of Hamiltonian type. Based on the ODE related to Φ^τ, we distinguish four model systems to be defined in (1.1) to (1.4).

The *Markovian model* systems arise from sequences written in the form $\{x_n\} = \{(q_n, z_n)\}_{n\in\mathbb{Z}^+}$ and given by

$$(q_{n+1}, z_{n+1}) = \Phi^\tau(q_n, \xi_n)\,, \tag{1.1}$$

where $\{\xi_n\}_{n\in\mathbb{Z}^+}$ is some i.i.d. sequence of random variables. Depending on the particular choice of $\{\xi_n\}$, we may generate different models. Embedded within the sequence $\{x_n\}$ is the reduced Markov chain for $\{q_n\}_{n\in\mathbb{Z}^+}$ given by

$$q_{n+1} = \Pi\Phi^\tau(q_n, \xi_n)\,, \tag{1.2}$$

where $\Pi : X \to \Omega$ denotes the projection onto Ω defined by $\Pi(q, z) = q$.

For the *non-Markovian model* systems we consider a family of flows Φ^t parameterized by ζ so that $\Phi^t(x) = \Phi^t(x; \zeta)$. We define the process $\{x(t)\} = \{(q(t), z(t))\}_{t\in\mathbb{R}^+}$ given by

$$(q(t), z(t)) = \Phi^t(q_0, \xi; \zeta)\,, \tag{1.3}$$

where ξ and ζ are random variables. Embedded within this is the reduced process for $\{q(t)\}_{t\in\mathbb{R}^+}$ given by

$$q(t) = \Pi\Phi^t(q_0, \xi; \zeta)\,. \tag{1.4}$$

The process (1.4) is not Markovian. It may, however, weakly approximate a Markov process for certain choices of the pair of random variables $\{\xi, \zeta\}$. In algorithmic practice we sample $\{q(t)\}_{t\in\mathbb{R}^+}$ at discrete time intervals to obtain a sequence $\{q_n\}_{n\in\mathbb{Z}^+}$ with $q_n = q(n\tau)$; this sampled process is not Markovian but may weakly approximate a Markov chain.

The Markovian construction (1.2) is of interest in molecular dynamics because it avoids the numerical simulation of long-term trajectories and the troublesome question of the sense in which such simulations are accurate. This Markovian reformulation of molecular dynamics was introduced in [19]. In (1.2) the maximal time interval is τ; however, there are situations where it is of interest to apply the transfer operator methodology to single long-term trajectories of a dynamical system; in this context, the non-Markovian construction (1.4) is of interest.

Reformulation of Key Questions

For both reduced model dynamics (1.2) and (1.4) we will consider situations where the sequence $\{q_n\}$ is approximately governed by sampling an SDE in time. The approximation will be controlled by the dimension of Z, improving as the dimension grows. The first three key questions can now be reformulated as follows:

(Q1) Based on observation of the full system processes (1.1) and (1.3), how can the reduced system be identified? Can identification by means of the transfer operator be justified for suitable model problems?

(Q2) How well do the metastable subsets and the flipping chains, calculated from the reduced systems (1.2) or (1.4), agree with the dynamics of the SDE that approximates the projected dynamics Πx_n from (1.1) or (1.3) in Ω?

(Q3) Assume that an SDE approximates the reduced dynamics from (1.1) or (1.3) on some state space $\hat{\Omega}$, but the projection Π maps onto a lower-dimensional subspace $\Omega \subset \hat{\Omega}$. In this situation there is memory in Πx_n, and it will not be close to Markovian in general. Which quantities are nonetheless accurately predicted by the algorithm, and which are not?

When studying (Q1) in the manner outlined above, we are considering application of the transfer operator approach to the dynamics in X and the determination of Π. In practice, when X is of very high dimension, this may not be feasible, and simpler identification strategies of Π may be required. Hence, when addressing (Q2) in the manner described above, we assume that Π is known and consider application of the transfer operator approach to the dynamics in Ω. We will not address question (Q4) in this paper, but leave it as a subject for future development; however, our analysis of question (Q3) suggests directions for this development.

Outline

In Section 2 we overview the basic algorithmic approach to macromolecular dynamics introduced in [20]. Simultaneously we establish the notation used throughout the paper. In Section 3 we describe the model problems of interest here. Sections 4, 5, and 6 contain our studies of questions (Q1), (Q2), and (Q3), respectively, using these model problems. Section 7 contains our conclusions, together with directions for further study.

2 Background

The extraction algorithm that we study here is built on the analysis of certain spectral problems arising in Markov chains. Hence we spend some time setting up the necessary background and notation.

Operators

We are given a discrete-time Markov chain $\{x_n\}$ on the state space X via its transition kernel $p = p(x, dy)$ with

$$p(x, A) = \mathbb{P}[x_1 \in A \mid x_0 = x] .$$

We define the *transfer operator* T, acting on bounded measurable functions $u : X \to \mathbb{R}$, via

$$(Tu)(x) = \int_X u(y)p(x, dy)\,.$$

Thus $(Tu)(x)$ is the expected value of u after one step of the chain started at x. If μ is an invariant measure of the Markov chain, then we define the *propagator* P, acting on μ-integrable functions $v : X \to \mathbb{R}$, by

$$\int_A (Pv)(y)\mu(dy) = \int_X v(x)p(x, A)\mu(dx)\,.$$

Hence P propagates functions v under the Markov chain.

To help orient the reader familiar with finite-state Markov chains $\{u_n\}$, we observe that, if S is a matrix with entries $S_{ij} = \mathbb{P}\{u_1 = j \mid u_0 = i\}$, then

$$T = S\,. \tag{2.1}$$

Let μ denote the (assumed positive and unique) invariant probability density, hence $S^{\mathsf{T}}\mu = \mu$. Then

$$P = D^{-1}S^{\mathsf{T}}D\,. \tag{2.2}$$

with $D = \mathrm{diag}(\mu)$. The observations (2.1) and (2.2) follow since S propagates expectations of functions and S^{T} propagates measures; equation (2.2) gives P, which just propagates measures normalized relative to μ. The Markov chain is *reversible* if $S^{\mathsf{T}}D = DS$. Note that then $P = S = T$ and S is self-adjoint with respect to the μ-weighted inner product $\langle a, b\rangle_\mu = a^{\mathsf{T}}Db$.

In the case of continuous state space we have to decide on which function space we want to study the operators T and P. For reversible Markov chains, we have the identity $P = T$ and their self-adjointness and hence real-valued spectrum in $L^2(\mu)$. In addition, $L^2(\mu)$ is also the space of choice from the viewpoint of numerics. In this paper we therefore restrict our attention to $L^2(\mu)$, whose corresponding 2-norm we denote by $\|\cdot\|_\mu$. Note, however, that there are interesting issues that arise in this context by considering other function spaces such as $L^1(\mu)$ and L^∞; see [11].

Most of the subsequent considerations will require that the dominant part of the spectrum (that part closest to 1) contain isolated eigenvalues of finite multiplicity only, so we will need some bound on the essential spectrum of P, i.e., the part of the spectrum other than isolated eigenvalues of finite multiplicity. All reversible Markov chains in the following meet this requirement [11]; in the nonreversible cases we simply *assume* that the essential spectrum is bounded away from the dominant spectrum. In the case of a continuous-time Markov process $\{X_t\}$, we often fix some observation time span $\tau > 0$ and consider the Markov chain $\{x_n\}$ found by sampling the Markov process at rate τ, i.e., $x_n = X_{n\tau}$.

Metastability

For quantifying metastability, we introduce a transition probability between subsets that measures the *dynamical fluctuations within the stationary ensemble* μ. To be more precise, define the transition probability $p(B, C)$ from B to C within one step as the conditional probability

$$p(B, C) = \mathbb{P}_\mu[x_1 \in C \mid x_0 \in B] = \frac{1}{\mu(B)} \int_B p(x, C)\mu(\mathrm{d}x)\,, \tag{2.3}$$

where $\mathbb{P}_\mu$ indicates that the Markov process has initial data distributed as μ; hence $\mathbb{P}_\mu[x_0 \in B] = \mu(B)$ for every B. An invariant set C is characterized by $p(C, C) = 1$, while an almost-invariant or metastable set can be characterized by $p(C, C) \approx 1$. Denoting by 1_A the indicator function of the subset A, the following important relation holds:

$$p(B, C) = \frac{\langle 1_C, P1_B\rangle_\mu}{\langle 1_B, 1_B\rangle_\mu}\,, \tag{2.4}$$

which is a straightforward consequence of the definition of P and equation (2.3).

Identification Strategy

The basic approach employed in [5, 20] for identifying metastable conformations in biomolecular systems can now be outlined for the model (1.1) and its embedded Markov chain (1.2). Note that the sequence $\{q_n, z_n\}$ is Markovian here, as is the embedded sequence $\{q_n\}$. We will use the notation P for the propagator corresponding to the full system (1.1) and P_q for the propagator corresponding to the reduced system (1.2). Similar ideas are employed for the non-Markovian model (1.3) and (1.4); indeed, algorithmically we proceed as if (1.4) is a Markov chain. In identifying metastable subsets, we employ the following *algorithmic strategy*:

> Metastable subsets can be identified via eigenfunctions of the propagator P corresponding to eigenvalues $|\lambda| < 1$ close to the dominant eigenvalue $\lambda = 1$.

Thus there is an assumption of a separation of time scales in the Markov chain; it is manifest in a spectral gap separating eigenvalues close to 1 and the remainder of the spectrum. This strategy was proposed by Dellnitz and Junge [4] for discrete dynamical systems with weak random perturbations and has been successfully applied to molecular dynamics in different contexts [5, 7, 20].

In what follows we give a mathematical justification for the algorithmic strategy and then follow this with two illustrative examples. Suppose that P is a self-adjoint propagator with spectrum satisfying

$$\sigma(P) \subset [l, r] \cup \{\lambda_2\} \cup \{1\}$$

and ordered so that $|\lambda_j| \le |\lambda_{j-1}|$. We assume that

$$-1 < l \le r = \lambda_3 < \lambda_2 < \lambda_1 = 1$$

so that λ_2 is a simple isolated eigenvalue. Furthermore, we assume that the eigenfunction v_2 corresponding to λ_2 is normalized so that $\langle v_2, v_2\rangle_\mu = 1$ and satisfies $v_2 \in L^\infty(\mu)$. In this setup we will obtain a decomposition into two metastable subsets; for generalizations to more than two metastable subsets, see [11]. In order to decompose $\mathbf{X}$ into two subsets $\mathcal{D} = \{B, C\}$, we define the following function:

$$v_{BC} = \sqrt{\frac{\mu(C)}{\mu(B)}}\, 1_B - \sqrt{\frac{\mu(B)}{\mu(C)}}\, 1_C\,. \tag{2.5}$$

This is constant on either of the two sets B and C and is normalized to $\|v_{BC}\|_2 = 1$. Under the assumptions on the propagator P stated above, we obtain the following relation between the existence of metastable subsets and eigenvalues close to 1:

THEOREM 2.1 [11] *Let $\mathcal{D} = \{B, C\}$ be an arbitrary decomposition of $\mathbf{X}$ into two subsets. Then*

$$1 + \kappa\lambda_2 \le [p(B, B) + p(C, C)] \le 1 + \lambda_2\,, \tag{2.6}$$

with $\kappa = \langle v_2, v_{BC}\rangle_\mu^2 \le 1$. In addition, choosing

$$B = \{x \in \mathbf{X} : v_2(x) \ge 0\} \quad \textit{and} \quad C = \{x \in \mathbf{X} : v_2(x) < 0\}\,,$$

we have $1 - 8c^2\epsilon \le \kappa$ with constants $\epsilon = (1 - \lambda_2)/(1 - \lambda_3)$ and $c = \|v_2\|_\infty$.

If the quantity $m = p(B, B) + p(C, C)$ is close to 2 (so that $p(B, B)$ and $p(C, C)$ are both close to 1), then metastability occurs. Theorem 2.1 highlights the strong relation between a decomposition of the state space into two metastable subsets and the presence of a second eigenvalue close to the dominant eigenvalue 1. The first part of Theorem 2.1 states that the lower bound on m is close to the upper bound whenever the eigenfunction v_2 corresponding to λ_2 is almost constant on the two metastable subsets B and C. This fact is exploited by the numerical identification algorithm. The second part of Theorem 2.1 quantifies this further, showing that m is close to 2 whenever (i) λ_2 is close to 1 and (ii) the gap between the second and third eigenvalue is large so that $\epsilon = (1 - \lambda_2)/(1 - \lambda_3)$ is small relative to the scale set by c. However, numerical experiments indicate that the identification strategy can be successful in situations where ϵ is not small [7].

To illustrate the identification strategy further we give two examples that generalize the preceding discussion to examples where there are two eigenvalues close to 1.

Example 1. Consider the three-well potential V illustrated in Figure 2.1 (left) with canonical invariant measure μ given by $\mu(dx) = \rho_{\text{can}}(x)dx$. This is the invariant density for the internal dynamics given by the Smoluchowski equation (3.3) with $f = -V'$ and $\beta\sigma^2 = 2$. We choose $\tau = 1$ as the observation time span, break the state space $\mathbb{R}$ into a large number of finite states (intervals), and study

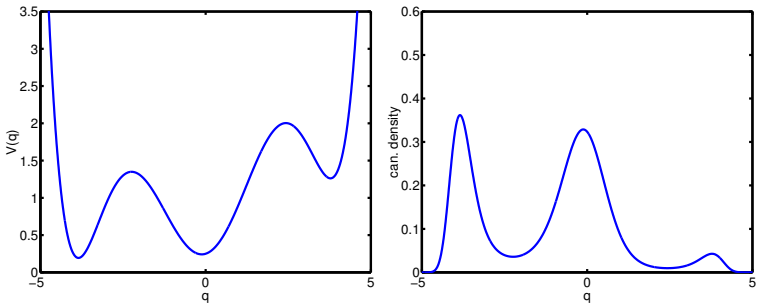

FIGURE 2.1. Three-well potential (left) and corresponding canonical density ρ_{can} for $\beta = 2$ (right).

the Markov chain $\{q_n\}$ given by $q_n = Q(n\tau)$.[1] Intuitively, we would expect to find three metastable subsets around the (local) minima of the potential function. The ordered spectrum of the propagator P looks as follows:

λ_1	λ_2	λ_3	λ_4	λ_5	λ_6	...
1.000	0.950	0.915	0.387	0.227	0.125	...

Notice the large spectral gap between λ_3 and λ_4. The first three eigenfunctions are shown in Figure 2.2. They exhibit a very special structure: They are almost constant around the local minima of the potential function V. This structure is exploited by the algorithm in order to identify the three metastable subsets [7].

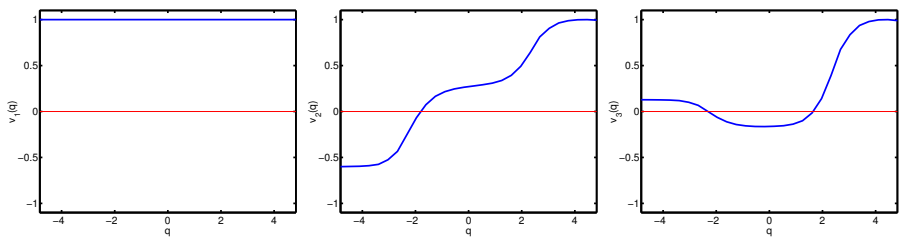

FIGURE 2.2. The three most dominant eigenfunctions of the propagator P for the Smoluchowski equation with $\beta = 2.0$ and $\gamma = 1.0$ corresponding to the eigenvalues 1.000, 0.950, and 0.915.

Example 2. Assume that we are given a decomposable finite-state-space Markov chain whose transition matrix S has three noncommunicating classes. The matrix S will have three eigenvalues at 1 with the remainder inside a circle of radius $r < 1$. The eigenvectors of S identify the three noncommunicating classes. If a small perturbation, retaining the Markov structure and inducing irreducibility, is introduced,

[1]Here, and in subsequent numerical experiments, the transition probabilities in the Markov chain are identified by the maximum likelihood estimator: in this case simply counting the number of transitions from state i to j relative to the total number of transitions out of i.

then the spectrum of S or P features a single eigenvalue at 1, two nearby eigenvalues just less than 1, and the remainder separated from these three eigenvalues. The structure of the eigenvectors of S or P corresponding to the three largest eigenvalues will, by continuity, identify the structure of the three noncommunicating sets [7].

When viewed in terms of the propagator P, the structure of the eigenfunctions associated with eigenvalues near 1, and alluded to in both examples, is the partition into almost constant segments. For the (ergodic) perturbed chain, the sets become *metastable states*: The chain will spend a long time in them before leaving; effective low-dimensional Markov behavior can be found by examining transitions between these metastable sets.

Essential Degrees of Freedom

Having in mind an identification of essential degrees of freedom, we propose the following algorithmic strategy as formulated in [7, 21]: Solve the eigenvalue problem for the propagator and the dominant eigenvectors and eigenvalues. Define the essential degrees of freedom as those directions that are orthogonal to the directions in which the dominant eigenfunctions are almost constant.

Note that for real problems of interest, an embedded SDE, or other explicit stochastic model, will not be known. The aim of the algorithms in [7, 21] is to find such a model numerically. In this paper we apply the algorithms to models where we know what the embedded stochastic model is. In the next section we exhibit model problems with the property that the embedded stochastic model is known.

3 Model Problems

We study the following harmonic oscillator forced system of equations with $q, u_j \in \mathbb{R}$:

$$\dot{q} = f(q) + \sigma\alpha^{\ell} \sum_{j=1}^{N} u_j \,, \quad \ddot{u}_j + \omega_j^2 u_j = 0 \,. \tag{3.1}$$

The basic mechanism to derive SDEs from this setup is to choose the frequencies and the initial data for the harmonic oscillators such that the cumulative action given by

$$U_N(t) = \sum_{j=1}^{N} u_j(t)$$

approximates either white noise or some Ornstein-Uhlenbeck (OU) process. We will either choose the frequencies as integers, when we use truncated Fourier series approximations of noise, or randomly when we use Monte Carlo approximation of Fourier integral representations of noise. In the white noise case $\ell = 0$ and α plays no role. In the OU case $\ell = \frac{1}{2}$ and α is the inverse correlation time of the OU process. By introducing ℓ in this case we are able to scale the problem so

that the temperature remains constant as $\alpha \to \infty$ and the colored noise problem approaches the white noise limit (see Theorem 3.3).

For initial conditions we take $q(0) = q_0$, $u_j(0) = u_j$, and $\dot{u}_j(0) = v_j$ for $j = 1, 2, \ldots, N$. We introduce $\mathbf{x} = (q, \mathbf{u}, \mathbf{v})$ with $\mathbf{u}(0) := \mathbf{u}_0 = (u_1, u_2, \ldots, u_N)$, $\mathbf{v}(0) := \mathbf{v}_0 = (v_1, v_2, \ldots, v_N)$, and $\mathbf{w} = (\omega_1, \omega_2, \ldots, \omega_N)$. Further, let $\Phi^t : \mathbb{R}^{2N+1} \to \mathbb{R}^{2N+1}$ denote the solution operator for the system (3.1); hence $\mathbf{x}(t) = \Phi^t(\mathbf{x}(0))$.

To better reveal the basic idea of construction in the following, we rewrite the system of ODEs (3.1) as

$$\dot{q} = f(q) + \sigma\alpha^{\ell} U_N(t)\,, \quad U_N(t) = \sum_{j=1}^{N} u_j \cos(\omega_j t) + \frac{v_j}{\omega_j} \sin(\omega_j t)\,. \tag{3.2}$$

Let Π_q and $\Pi_{\mathbf{u}}$ denote the projections of $\mathbf{x}$ onto the q- and $\mathbf{u}$-coordinates, respectively.

3.1 Generating White Noise

Here $\ell = 0$, and we consider the case where the forcing of the harmonic oscillators will be shown to approximate white noise. In this paper we will motivate the approximations we use rather informally. For theorems in this area, see [12, 14, 23, 24]. In Sections 3.2 and 3.3, the white noise approximation will be achieved in two different ways. In the first we will use truncated Fourier series, and in the second we will use Monte Carlo approximation of Fourier integrals. In both cases, the q-dynamics in (3.2) is approximated by the Smoluchowski, or high-friction Langevin, equation

$$\dot{Q} = f(Q) + \sigma \dot{W}\,. \tag{3.3}$$

For fixed $\tau > 0$ the solution process $Q(t)$ of (3.3) defines via time-τ sampling a (discrete time) Markov chain $\{Q_m\}$ given by $Q_m = Q(m\tau)$.

3.2 Markovian Case

The design of U_N is based on a Fourier series expansion of white noise [12, 24]

$$\dot{W}(t) \approx U_N(t) = \sqrt{\frac{1}{\pi}}\,\eta_0 + \sqrt{\frac{2}{\pi}} \sum_{j=1}^{N-1} \cos(jt)\eta_j\,, \quad 0 \le t \le \pi\,,$$

with η_m i.i.d. standard Gaussian.

Note that $U_N(t)$ is a Gaussian process satisfying

$$\mathbb{E}U_N(t)U_N(0) = \frac{1}{\pi} + \frac{2}{\pi} \sum_{j=1}^{N} \cos(jt)\,.$$

This expression is proportional to a Fourier truncation of the formal Fourier cosine series for a delta function and motivates the fact that $U_N(t)$ approximates a white noise.

In view of equation (3.2), we choose the following frequencies $\omega_j = (j-1)$ and random initial conditions for the harmonic oscillators:

$$\mathbf{v}_0 = \mathbf{0}\,, \quad \mathbf{u}_0 = \left(\sqrt{\frac{1}{\pi}}\,\eta_0, \sqrt{\frac{2}{\pi}}\,\eta_1, \sqrt{\frac{2}{\pi}}\,\eta_2, \dots\right), \tag{3.4}$$

with η_j i.i.d. and $\eta_1 \sim \mathcal{N}(0,1)$. Since the frequencies ω_j are rationally related and the construction is periodic, it is necessary to rerandomize the data every τ time units to avoid the periodicity inherent in such a construction. Thus, we choose the Markovian case (1.2) given by

$$q_{m+1} = \Pi_q \Phi^\tau(q_m, \mathbf{u}_m, \mathbf{v}_m) \tag{3.5}$$

with initial condition $q_0 \in \mathbb{R}$ and $\{\mathbf{u}_m, \mathbf{v}_m\}_{m\in\mathbb{Z}^+}$ an i.i.d. sequence of random variables distributed as (3.4). The relationship between the two Markov chains q_m and Q_m is contained in the following theorem. Because a pathwise construction of Brownian motion can be built from integrals of the Fourier series for white noise, it is possible to put both Q_m and q_m on the same probability space (see [13]) and hence the pathwise nature of the following theorem. Here *geometric ergodicity* refers to exponential convergence in time of expectations of measurable functions, bounded by quadratics, to their value under the invariant distribution.

THEOREM 3.1 *Let $f : \mathbb{R} \to \mathbb{R}$ be globally Lipschitz, let q_m be given by* (3.5)*, and let $Q_m = Q(m\tau)$ where Q solves* (3.3)*. Then there exists a constant $R > 1$ such that*

$$\mathbb{E}|q_m - Q_m|^2 \le \frac{R^m}{N}\,.$$

Furthermore, under the coercivity Assumption A.3 *on f (see Appendix* A*), both Markov chains are geometrically ergodic.*

PROOF: See Appendix A. □

3.3 Non-Markovian Case

Now the randomly chosen initial condition of the harmonic oscillators are based on Monte Carlo approximation of the Fourier integral representation of Brownian motion (see [16, sec. 6] for related issues). Brownian motion $W(t)$ can be written as a stochastic integral:

$$W(t) = \sqrt{\frac{2}{\pi}} \int_0^\infty \frac{1}{\omega} \sin(\omega t)\mathrm{d}B(\omega)\,,$$

where B is a standard Brownian motion. To see this, note that $W(t)$ is clearly a Gaussian process and that

$$\mathbb{E}W(t)W(s) = \frac{2}{\pi}\int_0^\infty \frac{1}{\omega^2}\sin(\omega t)\sin(\omega s)d\omega = \min(s,t)\,.$$

A calculation with, for example, Maple will show this is true. This motivates trying to approximate the following formal expression for white noise:

$$\dot{W}(t) = \sqrt{\frac{2}{\pi}} \int_0^\infty \cos(\omega t)\, \mathrm{d}B(\omega)\,, \tag{3.6}$$

Here B is a standard Brownian motion. Truncating the integral to $[0, N^a]$ and choosing N frequencies at random with average spacing N^{a-1} leads to the approximation

$$U_N(t) \approx \sqrt{\frac{2}{\pi}} \sum_{j=1}^{N} \cos(\omega_j t)\eta_j\,, \quad t \geq 0\,, \tag{3.7}$$

with frequencies

$$\omega_j \text{ i.i.d., } \omega_1 \sim \mathcal{U}(0, N^a)\,, \quad \eta_j \text{ i.i.d., } \eta_1 \sim \mathcal{N}(0, N^{a-1})\,, \tag{3.8}$$

for some $a \in (0, 1)$. It will be convenient to introduce the i.i.d. sequence $\nu = (\nu_1, \nu_2, \ldots) \in [0, 1]^{\mathbb{Z}^+}$ where $\nu_1 \sim \mathcal{U}(0, 1)$. Then we choose $\omega_j = N^a \nu_j$. Note that, for fixed frequencies $\{\omega_j\}$, $U_N(t)$ is a Gaussian process satisfying

$$\mathbb{E}U_N(t)U_N(0) = \frac{2}{N^{1-a}\pi} \sum_{j=1}^{N} \cos(\omega_j t) \approx \frac{2}{\pi} \int_0^{N^a} \cos(\omega t) d\omega\,.$$

Thus U_N has autocorrelation which is a Monte Carlo approximation to a truncation of the formal Fourier cosine integral for a delta function; this motivates the fact that $U_N(t)$ approximates a white noise.

In view of equations (3.2) and (3.7), we choose the random initial conditions

$$\mathbf{v}_0 = \mathbf{0}\,, \quad \mathbf{u}_0 = \left(\sqrt{\frac{2}{\pi}}\,\eta_1, \sqrt{\frac{2}{\pi}}\,\eta_2, \cdots\right) \tag{3.9}$$

for the harmonic oscillators. The resulting approximation is not periodic and hence is valid on any time interval. We are in the non-Markovian situation (1.4) given by

$$q(t) = \Pi_q \Phi^t(q_0, \mathbf{u}_0, \mathbf{v}_0; \mathbf{w}) \tag{3.10}$$

with initial condition $q_0 \in \mathbb{R}$ and random data given by (3.8) and (3.9).

In the Markovian case considered earlier, the approximation is strong (pathwise). For the non-Markovian approximation we are considering here, weak convergence in $C([0, T], \mathbb{R})$ is natural [1]. The relationship between the process q_t and the Smoluchowski Markov process $Q(t)$ defined by (3.3) is contained in the following theorem. Here q is defined on the probability space determined by the random initial data; the frequencies are considered fixed in the sense that the convergence is almost sure with respect to the sequence ν, which then determines the frequencies. The solution of the SDE, Q, is defined on the space of Wiener paths driving it.

THEOREM 3.2 *Let $f : \mathbb{R} \to \mathbb{R}$ be globally Lipschitz. Then, almost surely with respect to ν, q given by* (3.10) *and Q solving the Smoluchowski SDE* (3.3) *satisfy*

$$q \Rightarrow Q$$

in $C([0,T],\mathbb{R})$ for any $T > 0$ as $N \to \infty$. That is, $\mathbb{E}[g(q)] \longrightarrow \mathbb{E}[g(Q)]$ as $N \to \infty$ for any continuous bounded function $g : C([0,T],\mathbb{R}) \to \mathbb{R}$.

PROOF: This can be proven by adapting the methods in [14]; see also [23]. □

Although this approximation result holds for any $T > 0$, we anticipate that the rate of convergence deteriorates with the length of the time interval $[0,T]$ being considered. However, numerical and analytical evidence for related problems (see [14]) suggests that q_t generates an empirical measure and autocorrelations that are close to those of the Smoluchowski SDE (3.3) (under appropriate conditions on f, such as those given in Assumption A.3).

3.4 Generating Colored Noise

Here $\ell = \frac{1}{2}$ and we consider the case where the forcing of the harmonic oscillators approximates an Ornstein-Uhlenbeck process:

$$U_N(t) \approx U(t) = \sqrt{\frac{2\alpha}{\pi}} \int_0^\infty \frac{\sin(\omega t)}{\sqrt{\alpha^2+\omega^2}}\, \mathrm{d}B(\omega)\,, \tag{3.11}$$

where B is a standard Brownian motion. The process $U(t)$ is Gaussian and

$$\begin{aligned}\mathbb{E}U(t)U(s) &= \frac{2\alpha}{\pi}\int_0^\infty \frac{\sin(\omega t)\sin(\omega s)}{\alpha^2+\omega^2}\, ds \\ &= \frac{1}{2}\big[\exp\{-\alpha|s-t|\} - \exp\{-\alpha|s+t|\}\big]\,.\end{aligned}$$

A calculation with, for example, Maple will reveal this fact. Thus $U(t)$ is the nonstationary Ornstein-Uhlenbeck process

$$\dot{U} = -\alpha U + \sqrt{\alpha}\dot{W}\,, \quad U(0) = 0\,.$$

As a consequence, the dynamics in (3.2) is approximated by the system of first-order SDEs

$$\dot{Q} = f(Q) + \sigma\sqrt{\alpha}U\,, \quad \dot{U} = -\alpha U + \sqrt{\alpha}\dot{W}\,. \tag{3.12}$$

Note that sampling Q does not give a Markov chain. It is necessary to sample (Q,U) together to obtain a Markov chain. For later use we transform the system of first-order SDEs into a stochastic integral differential equation (SIDE) for Q alone. This is done by solving for U and inserting the result into the Q equation. As a result, we get the SIDE

$$\dot{Q}(t) = f(Q(t)) + \sigma\sqrt{\alpha}U(0)\exp(-\alpha t) + \sigma\alpha\int_0^t \exp(\alpha(s-t))\,\mathrm{d}W(s)\,. \tag{3.13}$$

Here the integral term represents the *memory effects* of the system, which are related to the *correlation time* α^{-1}. The effect of memory is more pronounced for

small α and disappears as $\alpha \to \infty$; we investigate the ramifications of this fact in our experiments. The following theorem is important in this regard. The proof is a straightforward application of the theory in [15]; see also [17, sec. 4.5]. The process Q found by projecting the solution of the SDE (3.12) and the process Q given by the SIDE (3.13) are identical. We comment further on this in Section 6.

THEOREM 3.3 *Let f be globally Lipschitz. Then as $\alpha \to \infty$, Q_{SIDE} solving the SIDE* (3.13) *satisfies*

$$Q_{\mathrm{SIDE}} \Rightarrow Q_{\mathrm{Smol}}$$

in $C([0, T], \mathbb{R})$, any $T > 0$, where Q_{Smol} solves the Smoluchowski SDE (3.3).

3.5 Non-Markovian Case

We find ODEs that are approximated by the SDE (3.12) as follows. By techniques similar to those in [14] and [23], we find the following Monte Carlo approximation of the Fourier integral representation of the Ornstein-Uhlenbeck process U in (3.11) gives

$$U_N(t) = \sqrt{\frac{2\alpha}{\pi}} \sum_{j=1}^{N} \sin(\omega_j t)\left(\alpha^2 + \omega_j^2\right)^{-1/2} \eta_j \,, \quad t \geq 0 \,, \tag{3.14}$$

with ω_j i.i.d. distributed as $\mathcal{U}(0, N^a)$ and η_j i.i.d. distributed as $\mathcal{N}(0, N^{a-1})$ for some $a \in (0, 1)$. In view of equation (3.2), we choose

$$\nu_k \text{ i.i.d.} \,, \quad \nu_1 \sim \mathcal{U}(0, 1) \,, \quad \omega_k = N^a \nu_k \,, \tag{3.15}$$

and random initial conditions

$$\mathbf{u_0} = \mathbf{0} \,, \quad v_j = \sqrt{\frac{2\alpha}{\pi}} \left(\alpha^2 + \omega_j^2\right)^{-1/2} \eta_j \omega_j \,, \quad j = 1, 2, \ldots, N, \tag{3.16}$$

with η_k i.i.d. and $\eta_1 \sim \mathcal{N}(0, N^{a-1})$ for the harmonic oscillators. As before, the resulting approximation is not periodic and hence is valid on any time interval. We are in the situation (1.4) of a long-term simulation given by

$$q(t) = \Pi_q \Phi^t(q_0, \mathbf{u}_0, \mathbf{v}_0; \mathbf{w}) \tag{3.17}$$

with initial conditions $q_0 \in \mathbb{R}$ and random data given by (3.15) and (3.16). For the following theorem we have the same probabilistic setting as for Theorem 3.2.

THEOREM 3.4 *Let $f : \mathbb{R} \to \mathbb{R}$ be globally Lipschitz, let q solve* (3.17)*, and let Q solve the SIDE* (3.13)*. Then, almost surely with respect to ν,*

$$q \Rightarrow Q$$

in $C([0, T], \mathbb{R})$ for any $T > 0$, as $N \to \infty$.

PROOF: Modifying the techniques in [14] (see also [23]) shows that U_N from (3.14) converges weakly to U given by (3.11) in $C([0, T], \mathbb{R})$. Since the mapping from U_N to q in (3.2) is continuous from $C([0, T], \mathbb{R})$ into itself, the result follows. □

4 Theoretical Analysis of Models Problems

In this section we want to study the spectral relation between the propagators P and P_q defined in terms of the Markov chains x_n and q_n, respectively. We address (Q1) by showing that, in certain situations for the model problems under consideration, the transfer operator in X has eigenfunctions that are approximately constant in the Z-coordinate, thereby identifying the space Ω as containing the essential dynamics. These situations occur when the dynamics in Ω is metastable so that the transfer operator in Ω has eigenvalues close to 1.

Recall that the Markovian model systems arise from a Markov chain for $x_n = (q_n, z_n)$ given by $(q_{n+1}, z_{n+1}) = \Phi^\tau(q_n, \xi_n)$ (see (1.1)), where $\{\xi_n\}_{n\in\mathbb{Z}^+}$ is some i.i.d. sequence of random variables. Let us denote the corresponding stochastic transition function by $p = p(q, z, M)$, where

$$p : \Omega \times Z \times \mathcal{B}(\Omega \times Z) \to [0, 1]\,.$$

Note that due to the random choice of ξ_n, the transition function is actually independent of its second variable. Denote by μ the (assumed unique) invariant probability measure of p, i.e., $\int p(q, z, M)\mu(\mathrm{d}q,\ \mathrm{d}z) = \mu(M)$. Embedded within the Markov chain x_n is the reduced Markov chain for $\{q_n\}_{n\in\mathbb{Z}^+}$ given by $q_{n+1} = \Pi_q \Phi^\tau(q_n, \xi_n)$ (see equation (1.2)), where $\Pi_q : X \to \Omega$ denotes the projection onto Ω. Denote the corresponding stochastic transition function by $p_q = p_q(q, A)$, where

$$p_q : \Omega \times \mathcal{B}(\Omega) \to [0, 1]\,.$$

Denote the invariant probability measure of p_q by μ_q. The following two relations hold:

(1) The stochastic transition functions obey

$$p_q(q, A) = p(q, z, A \times B)$$

for arbitrary $z \in \mathbb{Z}$, $A \in \mathcal{B}(\Omega)$, and $B \in \mathcal{B}(Z)$, and

(2) the invariant measures satisfy

$$\mu_q(A) = \mu(A \times B) \tag{4.1}$$

for arbitrary $A \in \mathcal{B}(\Omega)$ and $B \in \mathcal{B}(Z)$.

The independence of p in its second component z implies the following spectral relation between the two propagators P and P_q associated with the full and reduced Markov chain, respectively.

THEOREM 4.1 *Suppose that the transition function $p : \Omega \times Z \times \mathcal{B}(\Omega \times Z) \to [0, 1]$ is independent of its second variable. Consider the propagators $P : L^2(\mu) \to L^2(\mu)$ and $P_q : L^2(\mu_q) \to L^2(\mu_q)$. Then*

(i) *every eigenfunction ψ of P gives rise to an eigenfunction ϕ of P_q that corresponds to the same eigenvalue and obeys $\phi = \mathbf{E}_q[\psi]$ with*

$$\mathbf{E}_q[\psi](q)\mu_q(\mathrm{d}q) = \int_Z \psi(q, z)\mu(\mathrm{d}q,\ \mathrm{d}z)\,;$$

(ii) *if ϕ is an eigenfunction of P_q corresponding to the eigenvalue λ, then λ is also an eigenvalue of P corresponding to an eigenfunction ψ that satisfies*

$$\|\psi - (\phi \otimes \mathbf{1}_Z)\|_\mu^2 \leq 1 - \lambda^2 .$$

Hence, whenever λ is close to 1, the associated eigenvector of P approximately has the form $\phi \otimes \mathbf{1}_Z$.

PROOF: See Appendix A.2. □

Thus, within a Markovian setting, the dominant eigenvectors of P_q correspond to eigenvectors for P with the same eigenvalues and that are almost constant with respect to the harmonic oscillator coordinates. Theorem 4.1 hence shows that, for our Markovian model problems, the algorithms we are studying uniquely determine the q-coordinate as essential. This addresses question (Q1) posed in the introduction for Markovian systems as it shows that, in principle, the transfer operator can be used to identify Π. We re-emphasize, however, that practical implementation of the transfer operator approach to the identification of essential coordinates may be computationally infeasible if naively applied directly in X (cf. comments in the introduction). We also emphasize that the above theorem makes no statements about the behavior of the transfer operator approach in X for non-Markovian simulations.

5 Numerical Study of Model Problems: White Noise Case

In this section we study the spectral properties of the Markov chain $\{Q_m\} = \{Q(m\tau)\}$ found by sampling the Smoluchowski SDE (3.3), and compare them with spectral properties of the (case 1) Markov chain $\{q_m\}$ from (3.5) and the (case 2) non-Markovian stochastic process $\{q_m\}$ obtained from a long-term simulation of (3.10). In both cases the sequence $\{q_m\}$ is approximated by the sampled solution of the SDE; hence it is of interest to understand how this approximation property manifests itself in the spectral properties of propagators. This goes to the heart of the numerical algorithm used in macromolecular modeling.

We will assume that the SDE is ergodic and use ρ_{can} to denote the density of the invariant measure for this SDE. We will use ρ_{fd} to denote the approximation to ρ_{can} found by finite difference approximation of the generator, and ρ_{emp} to denote empirical approximation of ρ_{can} through sampling of a single trajectory of an SDE or a stochastic process that it approximates.

For both the underlying SDE and the sequence generated in cases 1 and 2, we discretize phase space into a finite number of boxes (actually intervals here). In the first subsection we approximate the generator of the process directly on this finite partition, enabling us to study the effective dynamics of the SDE without the effect of sampling. Then, for both the SDE and for cases 1 and 2, we study a single long-term simulation and use an Ulam-like discretization to calculate a flipping chain

on the set of boxes. In case 1 we know from Theorem 3.1 that, under appropriate conditions on f, (3.5) is an ergodic Markov chain and the existence of the propagator follows from this; thus we might expect similar properties for the Ulam-like approximation found by discretizing phase space. In case 2 we have less underlying theory—the sequence does not even come from a Markov chain; nonetheless, we proceed algorithmically as if the sequence q_m were generated by an ergodic Markov chain. This is reasonable because the sequence is weakly approximated by solving an SDE (Theorem 3.2).

We write $f(q) = -V'(q)$. The Smoluchowski Markov process Q_t solving the SDE (3.3) is itself geometrically ergodic, as are the Markov chains Q_n found by sampling it at rate $\tau > 0$. The SDE and its embedded Markov chains have invariant measure μ given by, for $\beta = 2/\sigma^2$,

$$\mu(dq) = \rho_{\text{can}}(q)\mathrm{d}q \propto \exp\{-\beta V(q)\}\mathrm{d}q\,. \tag{5.1}$$

We numerically investigate the essential dynamical behavior of the harmonic oscillator forced model problem (3.1), in both cases 1 and 2, and compare this dynamical behavior to that of the limit SDE approximating them. Hence, we compare the corresponding metastable subsets and the flipping chain defined on them. In all numerical simulations we choose $\beta = \frac{9}{2}$ and

$$V(q) = \frac{1}{3}(q^2 - 1)^2 - \frac{1}{15}q + \frac{1}{10} \tag{5.2}$$

shown in Figure 5.1 (left); Figure 5.1 (right) shows the induced invariant density. We take $\tau = 0.5$ as the observation time span.

5.1 Smoluchowski Limit Equation

We start by analyzing the limit Smoluchowski equation directly because this enables us to quantify errors caused by replacing $\mathbb{R}$ with a finite number of boxes and errors caused by statistical sampling. Specifically, by comparing ρ_{can}, ρ_{fd}, and ρ_{emp}, we can quantify these errors.

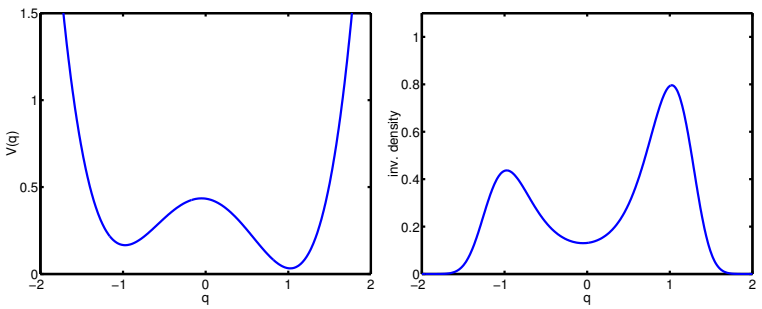

FIGURE 5.1. Potential function V used for tests and associated invariant density corresponding to the inverse temperature $\beta = 4.5$.

Recall that the propagator P_τ admits an infinitesimal generator in $L^2(\mu)$, i.e., $P_\tau = \exp(\tau\mathcal{L})$ with

$$\mathcal{L} = \frac{\sigma^2}{2}\frac{\partial^2}{\partial q^2} - V'(q)\frac{\partial}{\partial q}.$$

(Because the Markov process (3.3) is reversible, this is also the generator for the transfer operator T in this case.) It is well-known that the canonical density ρ_{can} (see (5.1)) is invariant for the Smoluchowski Markov process, that is, $\mathcal{L}^*\rho_{\text{can}} = 0$. Note that since $\beta = 2/\sigma^2$, we have $\sigma = \frac{2}{3}$. We discretize the generator $\mathcal{L}$ by means of second-order finite differences. The $L^1(\mathrm{d}x)$-error between the finite difference approximation of the invariant density of $\mathcal{L}^*$, ρ_{fd}, and the analytic solution ρ_{can}, as a function of the number of grid points, is shown in the following table:

# gridpoints	100	250	1000	2500	5000
$\|\rho_{\text{fd}} - \rho_{\text{can}}\|_1$	$1.09 \cdot 10^{-3}$	$1.72 \cdot 10^{-4}$	$1.07 \cdot 10^{-5}$	$1.71 \cdot 10^{-6}$	$4.27 \cdot 10^{-7}$
$\exp(\tau\gamma_2)$	0.9341	0.9341	0.9341	0.9341	0.9341
$\exp(\tau\gamma_3)$	0.4536	0.4533	0.4533	0.4533	0.4533

This table clearly shows second-order convergence in the number of grid points. Furthermore, it is clear that the first three eigenvalues γ_1, γ_2, and γ_3 of $\mathcal{L}$ are well approximated with as few as 250 grid points. Note that $\gamma_1 = 0$ in all cases. We have exponentiated the eigenvalue for direct comparison with eigenvalues of the propagator $P_\tau = \exp(\tau\mathcal{L})$. Figure 5.2 shows the structure of the eigenfunctions associated with the three leading eigenvalues. The piecewise constant structure of the second eigenfunction, together with the spectral gap between the second and third eigenvalue, indicates the presence of an embedded 2-state flipping chain.

Now we approximate the propagator P_τ by using a single realization of the Smoluchowski process sampled at rate $\tau = 0.5$. Recall that the propagator is constructed by using the maximum likelihood estimator (see Section 2). This allows us to study the influence of stochastic errors on the discretization. The $L^1(\mathrm{d}x)$-error between the empirical approximation to the invariant density ρ_{emp} of P_τ and the

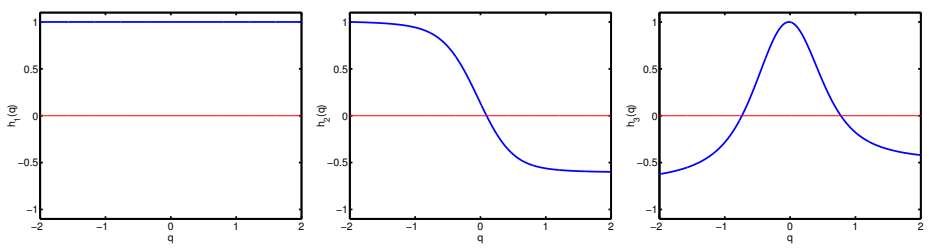

FIGURE 5.2. First, second, and third eigenfunction of the Smoluchowski generator $\mathcal{L}$ corresponding to the eigenvalues $\gamma_0 = 0.0000$, $\gamma_1 = -0.1363$, and $\gamma_2 = -1.5824$, respectively, discretized on $[-2, 2]$ with 1000 grid points.

analytic solution ρ_{can} is shown in the following table:

L	10000	50000	100000	300000	1000000
$\|\rho_{\text{emp}} - \rho_{\text{can}}\|_1$	0.0506	0.0161	0.0228	0.0107	0.0063

Here and below, the integer L is the number of samples in time used to approximate the transition probabilities. The number of boxes used is 30.

The next table shows the convergence of eigenvalues λ_k and eigenfunctions u_k of P_τ, the latter measured in the $L^2(\mu)$-distance to the eigenfunction h_k obtained from resolved finite difference approximation of the generator, as a function of the number of samples; note that we thus compare the λ_k with $\exp(\tau\gamma_k)$.

L	10000	50000	100000	300000	1000000	generator
λ_2	0.9370	0.9338	0.9332	0.9324	0.9328	0.9341
λ_3	0.4379	0.4494	0.4556	0.4504	0.4490	0.4533
$\|u_2 - h_2\|_2$	0.0348	0.0122	0.0263	0.0112	0.0050	–
$\|u_3 - h_3\|_2$	0.0442	0.0175	0.0126	0.0080	0.0049	–

The important point to notice is that, even for 10^4 samples, there is a close relationship with the results obtained by direct discretization of the generator. This suggests that the effect of sampling does not affect the qualitative results for $L = \mathcal{O}(10^4)$ or larger.

Based on the eigenfunctions of the propagator, we identify a decomposition of the state space $X = A \cup B$ with $A = (-\infty, 0.13]$ and $B = (0.13, \infty)$. Furthermore, we get the statistical weights $\mu(A) = 0.3947$ and $\mu(B) = 0.6053$, and the metastabilities $p(A, A) = 0.9251$ and $p(B, B) = 0.9511$. Hence the 2×2 stochastic matrix

$$S = \begin{pmatrix} 0.9251 & 0.0749 \\ 0.0489 & 0.9511 \end{pmatrix} \tag{5.3}$$

represents the flipping chain on the finite-state space given by the two states identified with the metastable subsets A and B.

5.2 ODEs with Random Data: Markovian Case

Now we compare the effective dynamical behavior of the harmonic-oscillator-driven system in the Markovian sample case (3.5) with the effective dynamical behavior of its limit Smoluchowski SDE (3.3).

For the experiments shown in the table below, the number of samples used is $L = 3 \times 10^5$. The integer N denotes the number of harmonic oscillators. The number of boxes/intervals used is 30. Now the u_j are eigenfunctions of the propagator for the oscillator-driven system calculated from a single sample path in time; λ_j are the corresponding eigenvalues. Now let ρ_{Smo} denote the canonical density corresponding to the Smoluchowski SDE (3.3), and h_j the eigenfunctions of the finite

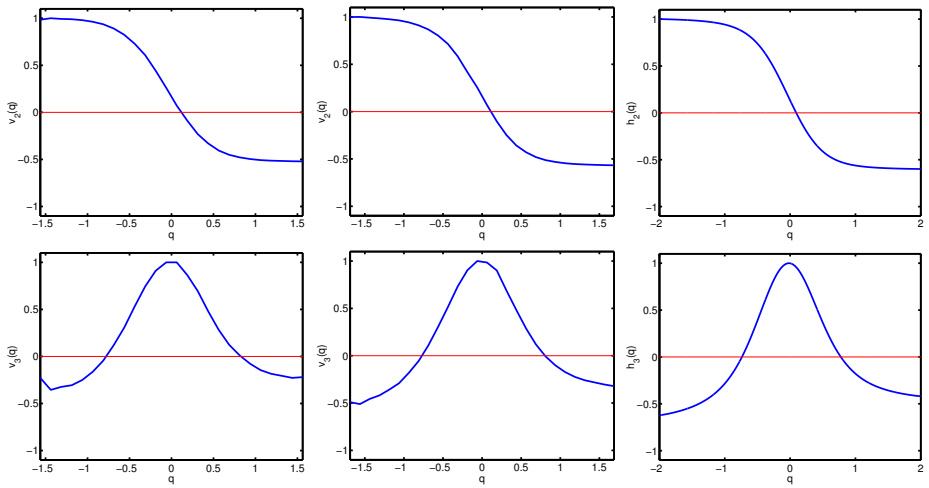

FIGURE 5.3. Second (top) and third (bottom) eigenfunctions of the Markovian white noise case for $N = 5, 10$ harmonic oscillators (left and middle) in comparison to the Smoluchowski eigenfunctions (right).

difference approximation of the propagator. (Later we will use ρ_{SIDE} to denote the canonical density for the SIDE (3.13).)

N	5	10	25	50	100	Smoluch.
$\|\rho_{\mathrm{emp}} - \rho_{\mathrm{Smo}}\|_1$	0.2471	0.1232	0.0442	0.0197	0.0070	–
$\|u_2 - h_2\|_2$	0.0548	0.0203	0.0104	0.0259	0.0301	–
$\|u_3 - h_3\|_2$	0.0705	0.0366	0.0133	0.0225	0.0223	–
λ_2	0.9572	0.9472	0.9387	0.9360	0.9331	0.9341
λ_3	0.4706	0.4587	0.4541	0.4500	0.4512	0.4533
$\mu(A)$	0.3541	0.3765	0.3883	0.3922	0.3925	0.3947
$\mu(B)$	0.6459	0.6235	0.6117	0.6078	0.6075	0.6053
$p(A, A)$	0.9471	0.9391	0.9306	0.9289	0.9253	0.9251
$p(B, B)$	0.9710	0.9632	0.9559	0.9541	0.9518	0.9511

Because of the small deviation of the second eigenfunctions, the metastable decompositions of the state space resulting from both the ODEs with random data for different N and from the Smoluchowski dynamics are in fact identical.

It is clear from this table and from Figure 5.3 that the algorithm performs excellently in identifying the correct metastable states—$\|u_2 - h_2\|_2$ is small—and identifying transition probabilities between them—$p(A, A)$ and $p(B, B)$ are close to the limiting SDE values. Combined with Theorem 4.1, which shows that the algorithm correctly identifies the projection Π, the table shows that the algorithm successfully and accurately finds a flipping chain approximating the dynamics of a large ODE system with periodically randomized data in a subspace. For example,

when $N = 100$, the governing 2×2 stochastic matrix for the flipping chain is

$$S = \begin{pmatrix} 0.9253 & 0.0747 \\ 0.0482 & 0.9518 \end{pmatrix},$$

which should be compared with (5.3). This answers question (Q2) of the introduction for the Markovian case.

As an aside it is noteworthy that, even for a very small number of oscillators (five or ten), the metastable sets and the flipping chain is approximated by the analogous dynamics for the SDE; see Figure 5.3 for further confirmation of this. For example, in the case $N = 5$, the 2×2 stochastic matrix for the flipping chain is

$$S = \begin{pmatrix} 0.9471 & 0.0529 \\ 0.0290 & 0.9710 \end{pmatrix},$$

which is reasonably close to that for the SDE limit, namely (5.3).

The form of constant-temperature molecular dynamics introduced in [19] is precisely of the above analyzed Markovian type: The momenta are periodically randomized according to the canonical distribution and a Markov chain in the position variables is thereby constructed. The experiments herein lend considerable weight to the methodology proposed in [19].

5.3 ODEs with Random Data: Non-Markovian Case

We carry out a similar analysis to that in the previous subsection, but now using the non-Markovian construction (1.4). Recall that we now take $q_n = q(n\tau)$ and study how well the metastable subsets and corresponding flipping chain resulting from the non-Markovian process can be approximated by those of the Smoluchowski process.

The approximation of the propagator P_τ is now based on a single long-term simulation of (3.10) for $a = (\frac{1}{3})$ and sampled at rate $\tau = 0.5$.[2] The results are summarized in the following table:

N	10	50	100	1000	5000	Smoluch.
$\|\rho_{\text{emp}} - \rho_{\text{Smo}}\|_1$	0.6031	0.3152	0.3610	0.1560	0.0621	–
$\|u_2 - h_2\|_2$	0.0495	0.0235	0.0653	0.0451	0.0231	–
$\|u_3 - h_3\|_2$	0.2022	0.0868	0.1109	0.1081	0.0570	–
λ_2	0.9934	0.9754	0.9759	0.9525	0.9421	0.9341
λ_3	0.8914	0.6896	0.6491	0.4964	0.4901	0.4533
$\mu(A)$	0.4056	0.3982	0.4279	0.4135	0.4003	0.3947
$\mu(B)$	0.5944	0.6018	0.5721	0.5865	0.5997	0.6053
$p(A, A)$	0.9855	0.9647	0.9687	0.9462	0.9337	0.9251
$p(B, B)$	0.9901	0.9766	0.9766	0.9621	0.9558	0.9511

[2]The choice $a = \frac{1}{3}$ is optimal for minimizing the difference from the SDE limit in this kind of approximation; see [14] for justification.

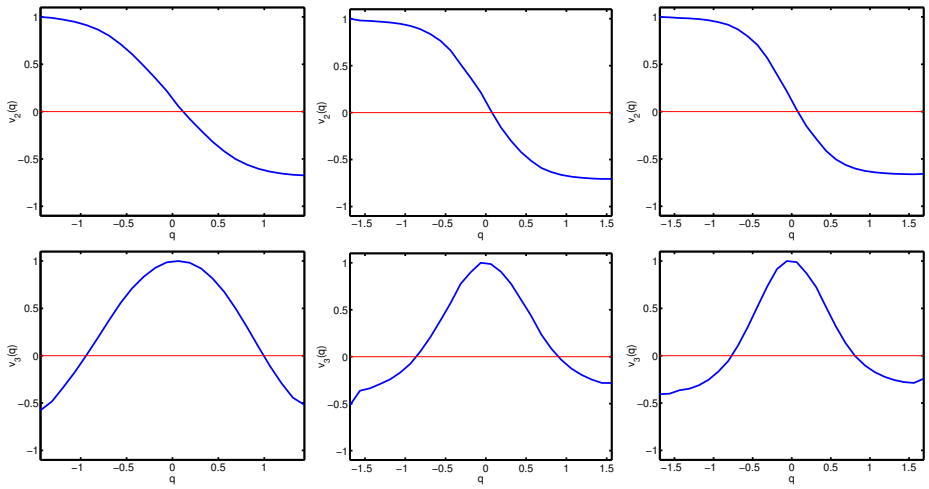

FIGURE 5.4. Second (top) and third (bottom) eigenfunctions of the Non-Markovian white noise case for $N = 10, 100, 1000$ harmonic oscillators (left to right).

As in the Markovian case, the metastable decomposition of the state space Ω is the same for all N and coincides with the metastable decomposition resulting from the Smoluchowski dynamics. It is important to realize that this table is generated by means of an algorithm which assumes that its input data, i.e., a sequence in discrete time, is Markovian. In this case the data $\{q_m = q(m\tau)\}$ is not Markovian, although $q(t)$ weakly approximates an SDE for N large (Theorem 3.2). Nonetheless, the algorithm correctly identifies the metastable subsets and the corresponding (Markovian) flipping chain from a single sample path of an ODE in $\mathbb{R}^{2N+1}$, with random initial data and parameters. This is further manifest in the eigenfunctions of the numerically generated transfer operator, which are shown in Figure 5.4 and which should be compared with those of the SDE itself in Figure 5.2. Notice the good agreement, even for quite small N, for the second eigenfunction; it is this eigenfunction that is used to partition state space. This gives an answer to the question (Q2) of the introduction in the non-Markovian case. Again, as in the Markovian construction in the previous section, the results are positive and lend weight to the ability of the algorithm to correctly identify macroscopic stochastic dynamics, in this case on the basis of a single long-term simulation of an ODE.

6 Numerical Study of Model Problems: Colored Noise Case

In this section we carry out numerical studies similar to those of the white noise case, but in the case where the driving noise is colored. Thus memory is significant. In this case the limiting dynamics that approximates our data solves the SIDE (3.13) or, equivalently, the Q part of the system of SDEs (3.12). We study spectral properties, metastable subsets, and resulting flipping chains corresponding

to the SIDE/SDE itself in Section 6.1 and compare them to those of the reduced harmonic-oscillator-driven process (3.17) in Section 6.2. Both these subsections are aimed at studying an algorithm that is predicated on the assumption of Markovian input data in the case where the data has memory. It is of interest to know how this memory is manifest in the transfer operator approach. In Section 6.3 we study the transfer operator approach in (Q, U)–space in order to show when, and how, the effect of memory is apparent. Throughout this section the choice of the potential V is as in the previous section.

6.1 Limit SIDE/SDE

We approximate the propagator P_τ corresponding to the SIDE (3.13) based on a single realization sampled at rate $\tau = 0.5$. As in previous numerical experiments, we choose $\sigma = \frac{2}{3}$, a discretization of the state space into 30 boxes and a sampling length of $L = 3 \times 10^5$ points. We analyze the system for different correlation decay rates $\alpha = 1, 6, 10, 20$. To circumvent the (numerical) problems involving the memory term of the SIDE (3.13), we exploit the relation between the SIDE and the system of SDEs (3.12) and sample the SDE in (Q, U) at rate $\tau = 0.5$, projecting the result onto Q: The first set of experiments (i) are thus based on the transfer operator approach applied to data found by projecting onto the Q-coordinate; we also study a second set (ii), conducted by applying the transfer operator approach to the pair (Q, U).

The following table gives information in case (i): We study the SIDE for different values of α and compare the results with those found from the Smoluchowski SDE that approximates it in the limit $\alpha \to \infty$ (see Theorem 3.3). The decomposition of the state space due to the second eigenfunction (see Figure 6.1) is given by $\Omega = (-\infty, 0.13] \cup (0.13, \infty)$, and is the same for all values of α chosen.

α	1.0	6.0	10.0	20.0	Smoluch.
λ_1	1.0000	1.0000	1.0000	1.0000	1.0000
λ_2	0.9946	0.9631	0.9524	0.9425	0.9341
λ_3	0.8197	0.5807	0.5271	0.4857	0.4533
$\mu(A)$	0.3011	0.3782	0.3828	0.3889	0.3946
$\mu(B)$	0.6989	0.6218	0.6172	0.6111	0.6053
$p(A, A)$	0.9869	0.9510	0.9411	0.9331	0.9251
$p(B, B)$	0.9944	0.9702	0.9635	0.9574	0.9511

The table clearly shows the convergence of the SIDE process to the Smoluchowski process for increasing α. Recall that the process obtained from sampling the SIDE is not Markovian; nonetheless, the flipping chains derived by *assuming* that the data is Markovian approximate the Smoluchowski flipping chain for large α. This reflects Theorem 3.3.

We observe qualitatively similar, but quantitatively different, behavior in case (ii): We discretize the propagator P_τ for the system of SDEs in (Q, U). We obtain

the following dominant spectrum of P_τ in dependence on α:

α	1.0	6.0	10.0	20.0	Smoluch.
λ_1	1.0000	1.0000	1.0000	1.0000	1.0000
λ_2	0.9841	0.9489	0.9423	0.9373	0.9341
λ_3	0.6118	0.4519	0.4533	0.4507	0.4533

6.2 ODEs with Random Data: Non-Markovian Case

In this section we study the reduced dynamics of the harmonic-oscillator-driven ODE (3.17) for increasing numbers N of harmonic oscillators and compare it to the dynamical behavior of the approximating SIDE—case (i) in the previous subsection. We focus on analyzing the effects of memory incorporated in the system via the decay rate of correlation α. To do so, we exploit long-term simulations according to equation (3.17) with $a = \frac{1}{3}$ and sampled at fixed rate $\tau = 0.5$ for different values of α. As in all other numerical experiments, we choose $\sigma = \frac{2}{3}$, a discretization of the state space into 30 boxes and a sampling length of $L = 3 \times 10^5$ points. In order to analyze the effects of memory, we choose two different values of α, namely 1.0 and 10.0, resulting in a decay of correlation given by $\exp(-\tau\alpha) = 0.61$ and $\exp(-\tau\alpha) = 0.007$, respectively. The following tables compare the reduced dynamics of the ODE (3.2), random initial data given by equation (3.16), with its approximating limit equation, the SIDE (3.13).

We start by studying the case $\alpha = 1.0$. As in the white noise case, eigenvalues and eigenfunctions of the propagator corresponding to the reduced ODE with

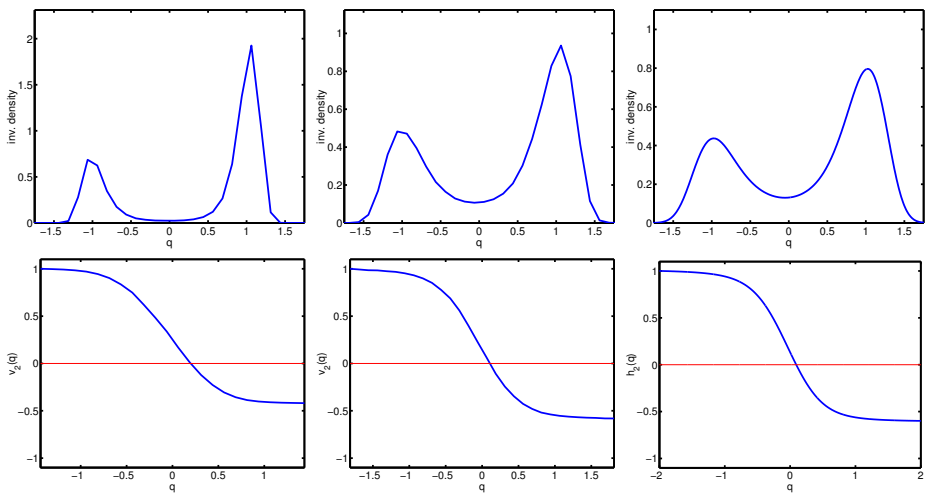

FIGURE 6.1. Comparison of SIDE for $\alpha = 1.0$ (left) and $\alpha = 10.0$ (middle) to Smoluchowski (right): invariant densities (top) and second eigenfunctions (bottom) of the corresponding propagators P_τ for SIDE and Smoluchowski equations.

random data are compared in the $L^2(\mu)$-norm to those of the limit dynamics, in this case the dynamics of the SIDE. Here, the function ρ_{SIDE} denotes the canonical density corresponding to the SIDE, which we find empirically.

$\alpha = \mathbf{1}$: N	25	50	100	500	1000	SIDE
$\|\rho_{\mathrm{emp}} - \rho_{\mathrm{SIDE}}\|_1$	0.6409	0.7172	0.4582	0.4533	0.5461	–
$\|u_2 - h_2\|_2$	0.1819	0.1375	0.1889	0.1204	0.1194	–
$\|u_3 - h_3\|_2$	0.3635	0.3377	0.4222	0.4112	0.3742	–
λ_2	0.9948	0.9964	0.9867	0.9862	0.9908	0.9946
λ_3	0.8568	0.8394	0.8463	0.8304	0.8315	0.8197
$\mu(A)$	0.4032	0.3763	0.4197	0.3831	0.3766	0.3011
$\mu(B)$	0.5968	0.6237	0.5803	0.6169	0.6234	0.6989
$p(A, A)$	0.9887	0.9919	0.9735	0.9715	0.9806	0.9869
$p(B, B)$	0.9923	0.9951	0.9808	0.9823	0.9883	0.9944

We observe that, despite memory effects, the eigenvalues, metastable subsets, and resulting finite-state-space Markov chains produced by the algorithm applied to the ODE (projected) and the limit SIDE are quite similar.

In the next table we study the case where the correlation decay is much faster ($\alpha = 10.0$):

$\alpha = \mathbf{10}$: N	25	50	100	500	1000	SIDE
$\|\rho_{\mathrm{emp}} - \rho_{\mathrm{SIDE}}\|_1$	0.3243	0.2411	0.2839	0.1633	0.1430	–
$\|u_2 - h_2\|_2$	0.1027	0.0502	0.1480	0.0942	0.0691	–
$\|u_3 - h_3\|_2$	0.0731	0.0421	0.0756	0.0729	0.0462	–
λ_2	0.9730	0.9666	0.9609	0.9458	0.9495	0.9524
λ_3	0.6197	0.5604	0.5925	0.5675	0.5631	0.5271
$\mu(A)$	0.4273	0.4024	0.4535	0.4383	0.4215	0.3828
$\mu(B)$	0.5727	0.5976	0.5465	0.5617	0.5785	0.6172
$p(A, A)$	0.9658	0.9586	0.9546	0.9381	0.9407	0.9411
$p(B, B)$	0.9745	0.9721	0.9623	0.9517	0.9568	0.9635

The approximation of the eigenfunctions of the limit SIDE is better than in the case $\alpha = 1.0$; see also Figure 6.2. However, the transition probabilities of the two-state Markovian flipping chain are close to those of the limit SIDE for both values of α.

The two cases $\alpha = 1$ and $\alpha = 10$ both give positive insight regarding question (Q2) in the introduction. Although neither the reduced process nor the limiting process is Markovian, the eigenvalues, metastable subsets, and resulting finite-state-space Markov chains corresponding to either process, and analyzed via the corresponding propagators, are very similar. In the data presented so far the effect of memory is only seriously manifest in the relatively poor approximation of the third eigenfunction of the transfer operator in the case $\alpha = 1.0$, at least when compared to the case $\alpha = 10.0$. We conjecture that the value of N necessary to obtain good approximation of the ODE dynamics by the limit SIDE is higher for small values of α.

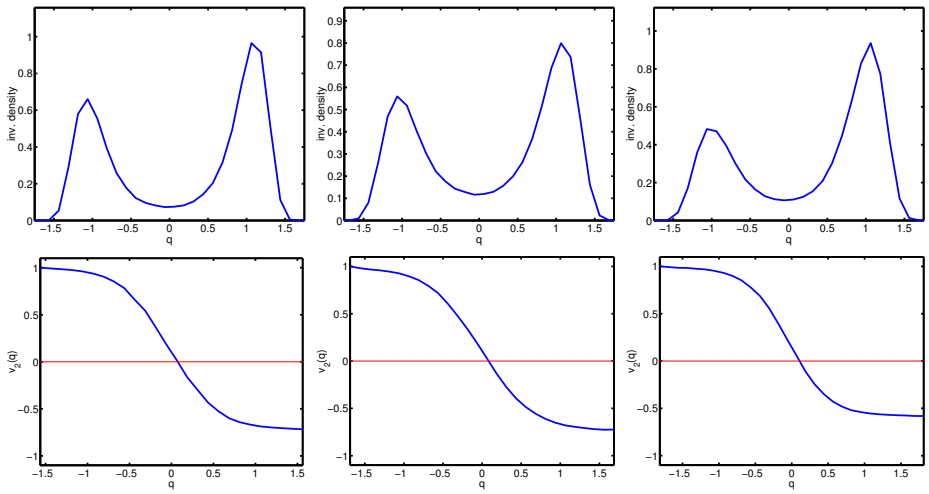

FIGURE 6.2. Comparison of the reduced harmonic oscillator forced ODE with random initial data for $N = 50$ (left) and $N = 500$ (middle) to approximating SIDE (right) for $\alpha = 10.0$: Invariant densities (top) and second eigenfunctions (bottom) of the corresponding propagators P_τ for ODEs and SIDE.

It is important to realize that in treating the limit SIDE as Markovian, which is how the final column (SIDE) is obtained in the preceding tables, we are committing a serious error—for α small this may lead to bad approximation of the effective behavior of the full system. The predictive capability of a Markovian approximation of the SIDE is likely to be severely compromised when α is not large. It is natural to ask, therefore, how this breakdown is manifest in the transfer operator approach and how it might be addressed. In the next section we indicate a manifestation of this issue. Developing the algorithm in order to deal with it will be the subject of further research.

6.3 ODEs with Random Data: Memory and the Transfer Operator Approach

In the previous subsection we studied eigenfunctions of the empirical transfer operator constructed by observing time series in $\mathbb{R}$ generated by the ODE system (3.1). We end up with the flipping chain identified above; this chain is close to that which is found based on observation of the SIDE (3.13), i.e., the correct Markovian limit behavior given by (3.12) projected onto the q-variable alone. However, these empirical transfer operators assume that the data is generated by a Markov chain, an assumption far from being true when α is not large. In real applications it is quite possible that such situations arise: The projected dynamics may have memory.

To illustrate how memory is manifest in the transfer operator approach, it is instructive to compare the eigenfunctions of the empirical transfer operator in $\mathbb{R}$

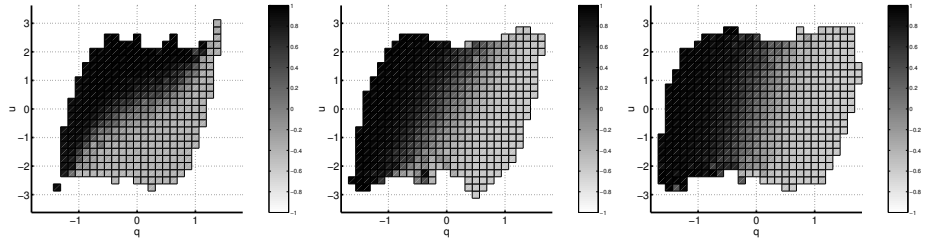

FIGURE 6.3. Second eigenfunctions of the propagator corresponding to the system of SDEs (3.12) for $\alpha = 1.0, 6.0, 20.0$ (from left to right).

for (3.1) with those of the SDE (3.12) in $\mathbb{R}^2$. In the latter case the observed time series in $\mathbb{R}^2$ *do* result from a Markov chain, and it is of interest to ask whether (i) the resulting metastable sets and (ii) the resulting effective dynamics are substantially different.

The eigenfunctions for (3.12) are functions of two independent variables. Figure 6.3 shows the second eigenfunction for $\alpha = 1.0, 6.0, 20.0$; the gray scale indexes constant-amplitude contours in the eigenfunction. Recall that our transfer operator approach to identifying essential dynamics exploits near constancy of the eigenfunctions. Figure 6.3 shows that for α large, when memory is negligible, partition of the state space on the basis of Q alone is reasonable—the eigenfunction is nearly constant in the U direction. For α smaller, however, it is clear that the natural decomposition requires knowledge of Q and U. Indeed, the natural decomposition into two states appears to be across the line $aQ + bU = c$ (approximately). This indicates that, if observation of both Q and U were available (equivalently both Q and $\dot{Q}$), the transfer operator methodology might produce significantly different results when memory is present. An investigation into the role of higher-order Markov models is therefore called for.

An important issue in this regard is the sampling rate relative to the correlation time of the noise. For a specific τ_* chosen such that $\alpha\tau_*$ is large enough, the limit dynamics in q as given by the SIDE (3.13) resembles a Markov process. For such a τ_*, the flipping chain based on time-τ_* samplings in q perfectly describes the statistics of flips between metastable sets on that time scale. Is it therefore natural to ask whether we should be content with studying the empirical transfer operator constructed by observing τ_*-time series in $\mathbb{R}$ generated by the ODE system (3.1)? We believe that the *effective dynamics* of the system should provide information about the family of flipping chains for the full range of sampling times τ. The effective dynamics is two-dimensional here, and the transfer operator approach will need to be extended to incorporate the memory effects in an optimal way.

7 Conclusions

The transfer operator approach for extracting the macroscopic dynamics of complex systems is an exciting new tool that has potential application in a variety of fields. The methodology has been applied in a variety of situations, and it is well motivated from a variety of standpoints. However, this is the first attempt to develop a rigorously founded systematic evaluation of the algorithm with respect to the problem of identification of, and projection onto, essential degrees of freedom in complex problems. We have done this by proposing a number of model problems, all motivated by the Kac-Zwanzig approach to the construction of a heat bath through harmonic oscillators. In these problems an ODE with random data, when projected onto a low-dimensional subspace, is approximated by an SDE. The work of Section 5, and to some extent Section 6, gives significant weight to the transfer operator algorithm, showing that it can correctly identify the essential degrees of freedom, and the corresponding finite-state-space Markov chain, embedded within some ODE of high dimension.

There are a number of directions for future development of this subject. The first is to study the effect of memory, touched upon in Section 6. The basic question here is whether we can use higher-order, or even hidden, Markov models to elucidate structure, such as that manifest in Figure 6.3, to derive increased predictive power for the transfer operator approach. The second direction for development is the study of Hamiltonian model problems, of the type proposed by Kac-Zwanzig, rather than the simple oscillator-driven problems considered here. A third direction is to develop new model problems more general than those of Kac-Zwanzig type to shed light on other problems in molecular dynamics and on problems outside this domain of application.

Appendix A: Convergence to SDE

Let $\{\eta_j^m\}$ with $j \in \{0, 1, \ldots, N\}$ and $m \in \mathbb{Z}^+$ be a doubly indexed set of i.i.d. random variables with $\eta_0^0 \sim \mathcal{N}(0, 1)$. Define $\mathbf{e}$ to be the vector $(1, 1, \ldots, 1) \in \mathbb{R}^{N+1}$.

Define $h_N(t)$ on $t \in [m\pi, (m+1)\pi)$ by

$$h_N(t) := \sum_{i=0}^{m-1} \eta_0^i \sqrt{\pi} + \frac{\eta_0^m (t - m\pi)}{\sqrt{\pi}} + \sum_{j=1}^{N-1} \sqrt{\frac{2}{\pi}}\, \eta_j^m \frac{\sin(j(t - m\pi))}{j}. \tag{A.1}$$

This gives a continuous approximation to Brownian motion on any time interval based on the fact that

$$\overline{W}(t) = W(t) - W(m\pi)$$

is a standard Brownian motion. Thus a Fourier sine series construction on $[0, \pi)$ can be repeated on $[m\pi, (m+1)\pi)$ by using a new set of independent random variables.

The following theorem extends a result from [2] for $t \in [0, \pi)$ to the arbitrary intervals considered above. The techniques of proof are based on ideas in [12, 13].

THEOREM A.1 *Consider $h_N(t)$ defined by* (A.1). *Then there is a Brownian motion on $\mathbb{R}^+$ such that, almost surely, $h_N(t) \to W(t)$ uniformly for $t \in [0, T]$, any $T > 0$, and we have that*

$$\sup_{t \in \mathbb{R}^+} \mathbb{E}|h_N(t) - W(t)|^2 \leq \frac{K}{N}.$$

Furthermore, if $T \in [m\pi, (m+1)\pi)$, then

$$\mathbb{E}\|h_N(\cdot) - W(\cdot)\|^2_{L^2(0,T)} \leq \frac{Cm}{N}.$$

Noting that $U_N = dh_N/dt$, we consider the ODE

$$\frac{dz}{dt} = f(z) + \sigma \frac{dh_N}{dt}, \quad z(0) = q_0, \tag{A.2}$$

and the SDE

$$dZ = f(Z) + \sigma dW, \quad Z(0) = Q_0. \tag{A.3}$$

Now $Q_m := Z(m\pi)$ defines a Markov chain on $\mathbb{R}$. We write this as

$$Q_{m+1} = G(Q_m, \omega_m), \tag{A.4}$$

where $\omega_m = \{W(t)\}_{t \in [m\pi, (m+1)\pi)}$. If

$$q_{m+1} = \mathcal{Q}\Phi^{\pi}(q_m, \mathbf{u}_m, 0),$$

then $q_m = z(m\pi)$ and $\{q_m\}_{m \in \mathbb{Z}^+}$ is also a Markov chain, approximating $\{Q_m\}_{m \in \mathbb{Z}^+}$. We write

$$q_{m+1} = G_N(q_m, \omega_m). \tag{A.5}$$

The fact that the two Markov chains are generated by the same noise sequence follows from the construction of Brownian motion through Fourier series. The relationship between the two Markov chains is contained in Theorem 3.1 whose first component is the following:

THEOREM A.2 *There exists an $R > 1$ such that*

$$\mathbb{E}|q_m - Q_m|^2 \leq \frac{R^m}{N}.$$

PROOF: Using the globally Lipschitz property of f gives

$$|G(a, \omega_m) - G(b, \omega_m)| \leq C|a - b|$$

where $C > 1$ is independent of a, b, N, and m; this is a straightforward SDE estimate. Theorem A.1 gives by a similar estimate using (A.2) and (A.3),

$$\mathbb{E}|G(a, \omega_m) - G_N(a, \omega_m)|^2 \leq \frac{\kappa}{N},$$

where $\kappa > 0$ is independent of a, N, and m. Combining the two estimates gives

$$\begin{aligned}\mathbb{E}|Q_{m+1} - q_{m+1}|^2 &\leq 2\mathbb{E}|G(Q_m, \omega_m) - G(q_m, \omega_m)|^2 \\ &\quad + 2\mathbb{E}|G(q_m, \omega_m) - G_N(q_m, \omega_m)|^2 \\ &\leq 2C\mathbb{E}|Q_m - q_m|^2 + 2\kappa N^{-1}\,,\end{aligned}$$

and the result follows. □

We now prove that the Markov chains (A.4) and (A.5) are geometrically ergodic under the following assumptions, which stand for the remainder of this section.

ASSUMPTION A.3 The function f satisfies:

- $f \in \mathbf{C}^2(\mathbb{R}, \mathbb{R})$;
- $\lim_{x\to\pm\infty} f(x) = \mp\infty$;
- $\exists \alpha, \beta > 0 : f(z) \leq \alpha - \beta z^2, \forall z \in \mathbb{R}$; and
- $\exists \gamma, \eta > 0 : |f(z)| \leq \gamma + \eta z, \forall z \in \mathbb{R}$.

Theorem A.4 establishes the second component of Theorem 3.1.

THEOREM A.4 *Under Assumption* A.3*, the Markov chains* (A.4) *and* (A.5) *are geometrically ergodic*: *There exists constants* $c > 0$ *and* $\Lambda > 1$ *such that, for all measurable* g *satisfying* $|g(x)| \leq x^2$*,*

$$|\mathbb{E}g(q_m) - \mu(g)| \leq \frac{C{q_0}^2}{\Lambda^n}\,,$$

where μ *is the unique stationary measure for the chain. An identical statement holds for the chain* $\{Q_m\}$.

PROOF: This follows from theorem 15.0.1 of [18]. Specifically, aperiodicity follows from the construction of the chains from SDEs and ODEs; the ψ-irreducibility and property that all compacts are petite follow from Corollary A.8. Condition 15.3 of [18] follows from Lemma A.5. □

The following is a straightforward consequence of Assumption A.3(iii):

LEMMA A.5 *The Markov chains* (A.4) *and* (A.5) *satisfy*

$$\mathbb{E}\big(|q_{m+1}|^2 \mid \mathcal{F}_m\big) \leq \lambda|q_m|^2 + R \tag{A.6}$$

and

$$\mathbb{E}\big(|Q_{m+1}|^2 \mid \mathcal{F}_m\big) \leq \lambda|Q_m|^2 + R\,, \tag{A.7}$$

where $R \in (0, \infty)$*,* $\lambda \in (0, 1)$*, and* $\mathcal{F}_m$ *is the* σ*-algebra of events up to and including the* m^{th}.

LEMMA A.6

$$\mathbb{P}(q_{m+1} \in B(0, \delta) \mid \mathcal{F}_m) > 0 \quad \forall \delta > 0\,, \tag{A.8}$$

$$\mathbb{P}(Q_{m+1} \in B(0, \delta) \mid \mathcal{F}_m) > 0 \quad \forall \delta > 0\,. \tag{A.9}$$

PROOF: We consider case (A.8) first. Let $\eta_j \equiv 0$ for $j \geq 1$. Then

$$\frac{dz}{dt} = f(z) + \frac{\sigma \eta_0}{\sqrt{\pi}}, \quad z(0) = q_0 .$$

Recall that $q_1 = z(\pi)$. A little thought shows that it is possible to choose η_0^* such that $q_1 = 0$. By choosing $(\eta_0, \eta_1, \ldots, \eta_N)$ to be in an ϵ-neighborhood of $(\eta_0^*, 0, \ldots, 0)$, we can ensure $q_1 \in B(0, \delta)$. Since the η_j's are Gaussian, this event has positive probability and we are done. □

In case (A.9) the result is proven by choosing the set of Brownian paths W close in the supremum norm topology to a control $\mathcal{U}$ such that

$$\frac{dZ}{dt} = f(Z) + \sigma \frac{d\mathcal{U}}{dt}, \quad Z(0) = Q_0, \ Z(\pi) = 0 .$$

LEMMA A.7 (i) *For any compact C,*

$$\mathbb{P}(q_{m+1} \in B(0, \delta) \mid \mathcal{F}_m) \geq \int_{y \in B(0,\delta)} \rho(q_m, y) dy ,$$

where $\rho(x, y)$ *is continuous in* $(x, y) \in C \times B(0, \delta)$ *and*

$$\inf_{(x,y) \in C \times B(0,\delta)} \rho(x, y) \geq \epsilon > 0 .$$

(ii)

$$\mathbb{P}(q_{m+1} \in A | \mathcal{F}_m) = \int_A \rho(q_m, y) dy ,$$

where $\rho(x, y)$ *is continuous in* $(x, y) \in \mathbb{R} \times \mathbb{R}$.

PROOF: (i) Define

$$\frac{dz}{dt} = f(z) + \frac{\eta_0}{\sqrt{\pi}} + \sum_{j=1}^{N} \sqrt{\frac{2}{\pi}} \eta_j \cos(jt), \quad z(0) = x .$$

$$\eta = (\eta_0, \eta_+), \quad \eta_+ = (\eta_1, \eta_2, \ldots, \eta_N), \quad G(\eta_0, \eta_+, x) = z(\pi) .$$

The equation of interest is $G(\eta_0, \eta_+, x) = y$. The result follows by using the invertibility of this equation for $\eta_0 = g(\eta_+, x, y)$ uniformly for $\eta_+ \in B(0, \epsilon)$, $x \in C$, and $y \in B(0, \delta)$.

(ii) This follows from the properties of nondegenerate diffusions.

□

In the language of [18], we have the following:

COROLLARY A.8 *The Markov chains* (A.4) *and* (A.5) *are* ψ*-irreducible* T*-chains and every compact set is petite.*

PROOF: The T-chain property [18, p. 127] follows by noting that Lemma A.7(i) can be generalized by replacing $B(0, \delta)$ with any measurable A, whilst Lemma A.7(ii) gives it directly for (A.5).

Combining this with Lemma A.6 gives ψ-irreducibility, by proposition 6.2.1 of [18]. Theorem 6.2.5(ii) of [18] implies that all compact sets are petite. □

Appendix B: Properties of Propagators and Transfer Operators

We prove Theorem 4.1, which states that the independence of the stochastic transition function p in its second component z implies strong spectral relation between the two propagators P and P_q associated with the full and reduced Markov chains, respectively.

THEOREM B.1 *Suppose that the transition function* $p : \Omega \times Z \times \mathcal{B}(\Omega \times Z) \to [0, 1]$ *is independent of its second variable. Consider the propagators* $P : L^2(\mu) \to L^2(\mu)$ *and* $P_q : L^2(\mu_q) \to L^2(\mu_q)$. *Then we have the following*:

(i) *Every eigenfunction* ψ *of* P *gives rise to an eigenfunction* ϕ *of* P_q *that corresponds to the same eigenvalue and obeys* $\phi = \mathbf{E}_q[\psi]$ *with*

$$\mathbf{E}_q[\psi](q)\mu_q(\mathrm{d}q) = \int_Z \psi(q, z)\mu(\mathrm{d}q, \mathrm{d}z) .$$

(ii) *If* ϕ *is an eigenfunction of* P_q *corresponding to the eigenvalue* λ, *then* λ *is also an eigenvalue of* P *corresponding to an eigenfunction* ψ *that satisfies*

$$\|\psi - (\phi \otimes \mathbf{1}_Z)\|_\mu^2 \leq 1 - \lambda^2 .$$

Hence, whenever λ *is close to* 1, *the associated eigenvector of* P *approximately has the form* $\phi \otimes \mathbf{1}_Z$.

PROOF: We first recall that the propagator P defined by

$$Pf(y, z)\mu(dy, dz) = \int_{\xi,\eta} f(\xi, \eta)p(\xi, \eta, dy, dz)\mu(d\xi, d\eta)$$

is bounded on $L^2(\mu)$ with $\|P\|_\mu = 1$. For any function $f = f(y, z)$ we define—for fixed y—the conditioned expectation $E_q : L^1(\mu) \to L^1(\mu_q)$ with respect to μ by integration with respect to z:

$$E_q[f](y)\mu_q(dy) = \int_Z f(y, z)\mu(dy, dz) . \tag{B.1}$$

In $L^2(\mu)$, the conditional expectation $E_q[f]$ acts as an orthogonal projection onto the space $U = \{g \otimes \kappa \mathbf{1}_Z : \kappa \in \mathbb{R},\ g \in L^2(\mu_q)\} \subset L^2(\mu)$ of square-integrable functions depending on y only. Any function $f \in L^2(\mu)$ can be decomposed into

$$f = (E_q[f]) \otimes \mathbf{1}_Z + \delta f , \tag{B.2}$$

with $\delta f \perp U$, i.e., $\langle \delta f, v \rangle_\mu = 0$ for every $v \in U$. In particular, we have $\langle (E_q[f]) \otimes \mathbf{1}_Z, \delta f \rangle_\mu = 0$. We now exploit the independence of P of η, property (4.1) of μ_q, and the definition $E_q[f]$ to perform the integration with respect to η, which yields

$$Pf(y,z)\mu(dy,\,dz) = \int\limits_\xi E_q[f](\xi)p(\xi,\cdot,dy,\,dz)\mu_q(d\xi)\,.$$

Since the right-hand side is also identical to $P(E_q[f] \otimes \mathbf{1}_Z)(y,z)\mu(dy,\,dz)$, we find that

$$Pf = P(E_q[f] \otimes \mathbf{1}_Z)\,. \tag{B.3}$$

This formula has two useful implications. First, inserting the decomposition (B.2) into (B.3) yields that

$$P\delta f = 0\,, \quad \text{i.e.,} \quad \delta f \in \ker(P)\,, \tag{B.4}$$

for any function f. Second, the definition of

$$P_q(E_q[f])(y)\mu_q(dy) = \int\limits_\xi (E_q[f])(\xi)p_q(\xi,\,dy)\mu_q(d\xi)$$

implies that

$$E_q[Pf] = P_q(E_q[f])\,. \tag{B.5}$$

As a consequence, every eigenvector ψ of P implies an eigenvector $E_q[\psi]$ of P_q corresponding to the same eigenvalue, since

$$P\psi = \lambda\psi \quad \Rightarrow \quad E_q[P\psi] = \lambda E_q[\psi] \quad \Rightarrow \quad P_q(E_q[\psi]) = \lambda E_q[\psi]\,.$$

Hence, assertion (i) is proved.

In order to show assertion (ii), we assume that $g \in L^2(\mu_q)$ is a normalized eigenvector of P_q, i.e., that $P_q g = \lambda g$ with $\|g\|_{\mu_q} = 1$. By denoting

$$h = P(g \otimes \mathbf{1}_Z) \in L^2(\mu)\,,$$

we observe that (B.5) implies $E_q[h] = E_q[P(g \otimes \mathbf{1}_Z)] = P_q g = \lambda\, g$ such that

$$h = \lambda g \otimes \mathbf{1}_Z + \delta h\,. \tag{B.6}$$

Since $P\delta h = 0$ due to (B.4), we immediately have that h is an eigenvector of P for the eigenvalue λ:

$$Ph = \lambda P(g \otimes \mathbf{1}_Z) + P\delta h = \lambda Ph\,.$$

Thus, to finally prove assertion (ii), we have to show that $\|\delta h\|_\mu^2 \leq 1 - \lambda^2$. To do so, we exploit (B.6) to observe that

$$\|h\|_\mu^2 = \langle h, h\rangle_\mu = \lambda^2 \langle g \otimes \mathbf{1}_Z, g \otimes \mathbf{1}_Z\rangle_\mu + \langle \delta h, \delta h\rangle_\mu + \langle g \otimes \mathbf{1}_Z, \delta h\rangle_\mu\,.$$

The first term equals λ^2, because g is normalized; the third term vanishes since $\delta h \perp U$, yielding

$$\|h\|_\mu^2 = \lambda^2 + \|\delta h\|_\mu^2\,.$$

However, due to $h = P(g \otimes \mathbf{1}_Z)$ and $\|P\|_\mu = 1$, we get $\|h\|_{2,\mu}^2 \leq 1$, which together with the above identity results in $\|\delta h\|_\mu^2 \leq 1 - \lambda^2$ as desired. □

Acknowledgments. We are grateful to A. J. Majda for encouraging the collaboration that led to this work. We are grateful to A. J. Majda, E. Vanden Eijnden, and P. F. Tupper for illuminating and insightful discussions. W. Huisinga was supported by "Deutsche Forschungsgesellschaft" within SPP 1095: "Analysis, Modeling and Simulation of Multiscale Problems." A. M. Stuart is supported by the EPSRC.

Bibliography

[1] Billingsley, P. *Convergence of probability measures*. Wiley, New York–London–Sydney, 1968.

[2] Cano, B.; Stuart, A. M.; Süli, E.; Warren, J. O. Stiff oscillatory systems, delta jumps and white noise. *Found. Comput. Math.* **1** (2001), no. 1, 69–99.

[3] Chorin, A. J.; Hald, O. H.; Kupferman, R. Non-Markovian optimal prediction. *Phys. D*, in press.

[4] Dellnitz, M.; Junge, O. On the approximation of complicated dynamical behavior. *SIAM J. Numer. Anal.* **36** (1999), no. 2, 491–515.

[5] Deuflhard, P.; Dellnitz, M.; Junge, O.; Schütte, C. Computation of essential molecular dynamics by subdivision techniques. *Computational molecular dynamics: challenges, methods, ideas. Proceedings of the 2nd International Symposium on Algorithms for Macromolecular Modelling held at the Free University of Berlin, Berlin, May 21–24, 1997*, 98–115. Lecture Notes in Computational Science and Engineering, 4. Springer, Berlin, 1999.

[6] Deuflhard, P.; Hermans, J.; Leimkuhler, B.; Mark, A. E.; Reich, S.; Skeel, R. D., eds. *Computational molecular dynamics: challenges, methods, ideas. Proceedings of the 2nd International Symposium on Algorithms for Macromolecular Modelling held at the Free University of Berlin, Berlin, May 21–24, 1997*. Lecture Notes in Computational Science and Engineering, 4. Springer, Berlin, 1999.

[7] Deuflhard, P.; Huisinga, W.; Fischer, A.; Schütte, C. Identification of almost invariant aggregates in reversible nearly uncoupled Markov chains. *Linear Algebra Appl.* **315** (2000), no. 1-3, 39–59.

[8] Fischer, A.; Schütte, C.; Deuflhard, P.; Cordes. F. Hierarchical uncoupling-coupling of metastable conformations. *Computational methods for macromolecules: challenges and applications—Proceedings of the 3rd International Workshop on Algorithms for Macromolecular Modelling*. Lecture Notes in Computational Science and Engineering. Springer, 2002.

[9] Ford, G. W.; Kac, M. On the quantum Langevin equation. *J. Statist. Phys.* **46** (1987), no. 5-6, 803–810.

[10] Freidlin, M. I.; Wentzell, A. D. *Random perturbations of dynamical systems.* Grundlehren der Mathematischen Wissenschaften, 260. Springer, New York, 1984.

[11] Huisinga, W. Metastability of Markovian systems: A transfer operator approach in application to molecular dynamics. Ph.D. thesis, Free University Berlin, 2001. Available at `http://www.math.fu-berlin.de/~huisinga/talks/Ascona0701.pdf`.

[12] Kahane, J.-P. *Some random series of functions*. Second edition. Cambridge Studies in Advanced Mathematics, 5. Cambridge University Press, Cambridge, 1985.

[13] Krylov, N.V. *Introduction to the theory of diffusion processes*. Translations of Mathematical Monographs, 142. American Mathematical Society, Providence, R.I., 1995.

[14] Kupferman, R.; Stuart, A. M.; Terry, J. R.; Tupper, P. F. Long term behaviour of large mechanical systems with random initial data. Preprint, 2002.

[15] Kurtz, T. G. A limit theorem for perturbed operator semigroups with applications to random evolutions. *J. Functional Analysis* **12** (1973), 55–67.

[16] Majda, A. J.; Kramer, P. R. Simplified models for turbulent diffusion: theory, numerical modelling, and physical phenomena. *Phys. Rep*. **314** (1999), no. 4-5, 237–574.

[17] Majda, A. J.; Timofeyev, I.; Vanden Eijnden, E. A mathematical framework for stochastic climate models. *Comm. Pure Appl. Math*. **54** (2001), no. 8, 891–974.

[18] Meyn, S. P.; Tweedie, R. L. *Markov chains and stochastic stability*. Communications and Control Engineering Series. Springer, London, 1993.

[19] Schütte, C. Conformational dynamics: modelling, theory, algorithm, and application to biomolecules. Habilitation thesis, Free University, Berlin, 1999. Available at `http://www.zib.de/bib/diss/cont.de.html`.

[20] Schütte, C.; Fischer, A.; Huisinga, W.; Deuflhard, P. A direct approach to conformational dynamics based on hybrid Monte Carlo. Computational molecular biophysics. *J. Comput. Phys*. **151** (1999), no. 1, 146–168.

[21] Schütte, C.; Huisinga, W. Biomolecular conformations as metastable sets of Markov chains. *Proceedings of the Thirty–Eighth Annual Allerton Conference on Communication, Control, and Computing, Monticello, Illinois*, 1106–1115. University of Illinois at Urbana-Champaign, 2000.

[22] Schütte, C.; Huisinga, W.; Deuflhard, P. Transfer operator approach to conformational dynamics in biomolecular systems. *Ergodic theory, analysis, and efficient simulation of dynamical systems*, 191–223. Springer, Berlin, 2001.

[23] Stuart, A. M.; Terry, J. R.; Tupper, P. F. *Constructing SDEs from ODEs with random data*. Stanford University Technical Report SCCM-01-04. Available at `http://www-sccm.stanford.edu/wrap/pub-tech.html`.

[24] Stuart, A. M.; Warren, J. O. Analysis and experiments for a computational model of a heat bath. *J. Statist. Phys*. **97** (1999), 687–723.

[25] Zwanzig, R. Nonlinear generalized Langevin equations. *J. Statist. Phys*. **9** (1973), 215–220.

WILHELM HUISINGA
Free University
Mathematik and Informatik
14195 Berlin
GERMANY
E-mail: `huisinga@math.fu-berlin.de`

CHRISTOF SCHÜTTE
Free University
Mathematik and Informatik
14195 Berlin
GERMANY
E-mail: `schuette@math.fu-berlin.de`

ANDREW M. STUART
University of Warwick
Mathematics Institute
Coventry CV4 7AL
UNITED KINGDOM
E-mail: `stuart@maths.warwick.ac.uk`

Received January 2002.